

PAPER NAME

Analysis of Mineral Sediment Characteristics of Bantimurung Bulusaraung National Park in the Karst

AUTHOR

Muhammad Arsyad

WORD COUNT

3536 Words

CHARACTER COUNT

16662 Characters

PAGE COUNT

8 Pages

FILE SIZE

1.0MB

SUBMISSION DATE

Dec 27, 2022 4:30 PM GMT+8

REPORT DATE

Dec 27, 2022 4:30 PM GMT+8

● **8% Overall Similarity**

The combined total of all matches, including overlapping sources, for each database.

- 8% Internet database
- 0% Publications database
- Crossref Posted Content database

● **Excluded from Similarity Report**

- Crossref database
- Submitted Works database
- Bibliographic material
- Quoted material
- Cited material
- Small Matches (Less than 10 words)
- Manually excluded sources

PAPER • OPEN ACCESS

4 **Analysis of mineral sediment characteristics of Bantimurung Bulusaraung National Park in the Karst Maros Region**

3 To cite this article: M Arsyad *et al* 2020 *J. Phys.: Conf. Ser.* **1572** 012007

View the [article online](#) for updates and enhancements.

You may also like

- 5 [Strategy to develop tourism objects at Ijobalit, a former pumice mine in East Lombok](#)
A Kurniawan, F Susanti and S R Yuniarti
- 2 [Study of soil management in rice fields in Bantimurung District Maros Regency](#)
D E Safitri, A Ahmad and M Nathan
- 2 [Strategy for the development of large scale rice milling industry in Maros Regency](#)
Salmah Desi, A.H Latief R. and Jamil Hatta



The Electrochemical Society
Advancing solid state & electrochemical science & technology

243rd ECS Meeting with SOFC-XVIII

More than 50 symposia are available!

Present your research and accelerate science

Boston, MA • May 28 – June 2, 2023

[Learn more and submit!](#)

4 Analysis of mineral sediment characteristics of Bantimurung Bulusaraung National Park in the Karst Maros Region

M Arsyad*, N Ihsan and V A Tiwow

Department of Physics, Universitas Negeri Makassar, Kampus UNM Parangtambung
Jl. Daeng Tata Raya, Makassar 90224, Indonesia

*E-mail: m_arsyad288@unm.ac.id

Abstract. Research has been carried out to describe the profile of the sediment layer and analyze the composition of sediment minerals in the former mine area of the Karst Maros area. Data is collected by measuring in the field in one of the former mining areas using a geoelectric tool. The measured data are current strength, voltage, and then an analysis is performed to obtain the value of resistance and resistance using the Wenner configuration. The results of the analysis were processed using Res2dinV software to obtain resistivity cross-sections in the measurement area. Processing results obtained by sedimentary profiles in the former mine area of the Maros Karst Area in the form of layers at resistivity values in the range of 0.17 Ωm to 7.80 Ωm and the corresponding types of material are groundwater, sand, clay, and limestone. The varying resistivity value is around a depth of up to 6 m. After this depth, the bedding will have almost the same material as hard limestone. While the mineral composition in the Karst Maros Region consists of chalcopyrite, galena, pyrite, pyrrhotite, magnetite, cassiterite, hematite, and clay.

1. Introduction

Karst areas have different characteristics from non-karst regions. The karst region is characterized by a heterogeneous medium and is very vulnerable to external pressure. The karst area is characterized [1] by 1) the presence of closed basins and/or dry valleys in various sizes and shapes, 2) the scarcity or absence of surface drainage/streams, and 3) the presence of caves from underground drainage systems. The availability of water in the karst area is determined by the amount of rainfall that can be accommodated during the rainy season and gives it to the surrounding environment during the dry season. The karst area of Maros, South Sulawesi is known as the karst type of tower (tower karst).

The Maros karst area has approximately 268 caves, 6 of which are upstream from the major rivers in South Sulawesi. The distribution of springs can be grouped into three parts, namely high spring density (> 5 caves/km²), medium spring density (2-5 caves/km²), and low spring density (< 2 caves/km²) (Oktariadi, 2009). While the largest aquifer potential is found at a depth of 12-15.7 m (groundwater/aquifer is suppressed because it is flanked by a layer of hard rock) and accumulates evenly in the rock layer [2].

The peak of rainfall occurs in December (717.30 mm) and January around (827.40 mm) [3]. The nature of rainfall causes hydrogeological conditions in the karst area to be easily disturbed [4] identified based on factors such as 1) porosity, 2) water content and hydraulic conductivity of



sediment fill, 3) water flow and spring response, and 4) water quality. These four conditions require porosity as one of the factors driving the availability of water in the karst region.

Maros Regency in South Sulawesi is between $40^{\circ}45'50''\text{LS}$ and $109^{\circ}20'00''\text{BT}$ to $129^{\circ}12'00''\text{BT}$. The area of Maros Regency is $1,619.12 \text{ km}^2$ with sedimentary rocks dominating its topography. Sedimentary rocks have a very important meaning to express the life characteristics of organisms because most human activities are on the surface of the earth. Fossils can also be found in sedimentary rocks and have important significance in determining rock age and depositional environment. Sedimentary rocks are rocks formed due to the process of diagnosis from other rock material that has undergone sedimentation. Sedimentation includes the processes of weathering, erosion, transportation, and deposition. The weathering process that occurs can be either physical or chemical weathering. The erosion and transportation processes are carried out by water and wind media. The deposition process can occur if the energy transport is not able to transport the particles.

Sedimentary rocks are identified based on the surface texture of the rough, medium and fine texture. Rough texture, occurs on the surface of the grain looks tapered and feels sharp. Medium texture occurs when the surface of the grain is slightly tapered to slightly flat. This texture is found on the grains with the level of roundness tapered responsibility to round responsibility. While smooth texture occurs if the surface of the grain is smooth and flat. This shows the surface aberration process of the grain that has been advanced when experiencing transportation. Thus sediment grains that have a smooth surface texture occur in rounded roundness to very rounded. The process of deposition of suspension can be described by the dependent load as the speed and turbulence of the flow decrease in a series of steps over a certain period time. At first, the flow energy is sufficient to transport all the particles in suspension and is deposited as a layer at the bottom of the river then, the flow energy drops even more, and medium-sized sand particle is stored on the second bottom under this flow. The accumulation of sediment particles in separate layers is called stratification. Stratification is one of the diagnostic characteristics of sedimentary rocks [5].

The sedimentation process continues and causes the land to become open land. This impact occurs as a result of stripping and overburden activities that cause the soil to stir and soil layers to change. This incident causes changes in the physical and chemical properties of the soil so that it can ultimately reduce the level of soil fertility. For this reason, an in-depth study of sedimentation needs to be carried out to maintain sustainable development under the heading of the analysis of the mineral characteristics of the Maros karst area in the Bantimurung Bulusaraung National Park.

2. Method

This research was conducted in two stages, namely: 1) measurement in the field, namely the location of the Maros karst area, around the former cement factory mine, and 2) data analysis in the Earth Physics Laboratory, Faculty of Mathematics and Natural Sciences, Makassar State University. The measured physical quantities are the potential difference (V), self-potential (V_{sp}), strong current (I), the distance of potential electrode, and distance of current electrode to determine resistance (R), geometry factor (K), and resistivity (ρ). This amount is measured using the geoelectric resistivity method.

Some stages of the acquisition are: 1) Measuring the distance of the stakes that will be used as far as 60 m for 21 stakes. 2) Installing stakes which are numbered (1-21) on the measurement track to make it easier to adjust the electrode stretch. 3) Adjust the current and potential electrode ranges for the first electrode spacing $a = 3 \text{ m}$ and $n = 1$, in this case, electrodes A on stakes 1, M on stakes 2, N on stakes 3, and B on stakes 4. 4) Perform data retrieval for the first datum point by following per under the workings of the tool. Flow data (I), potential (V), and self-potential (V_{sp}) are recorded in the acquisition format. 5) Each electrode is moved as far as 3 m following the line direction (electrode A is moved to M, M moves to N, and N to B), then re-measure the current strength, potential and self-potential for the second datum point, and so on until the electrode B until the peg 21. The stages are carried out using the Wenner configuration as in figure 1. Furthermore, the results obtained are

processed using the Res2DinV software to obtain a cross-sectional model of resistivity. The data processing steps can be seen in the following flow chart in figure 2.

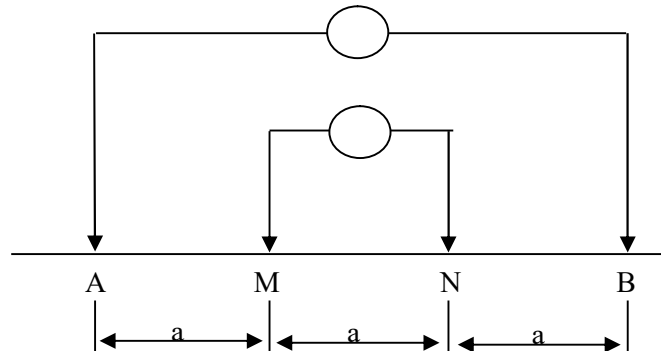


Figure 1. Wenner configuration.

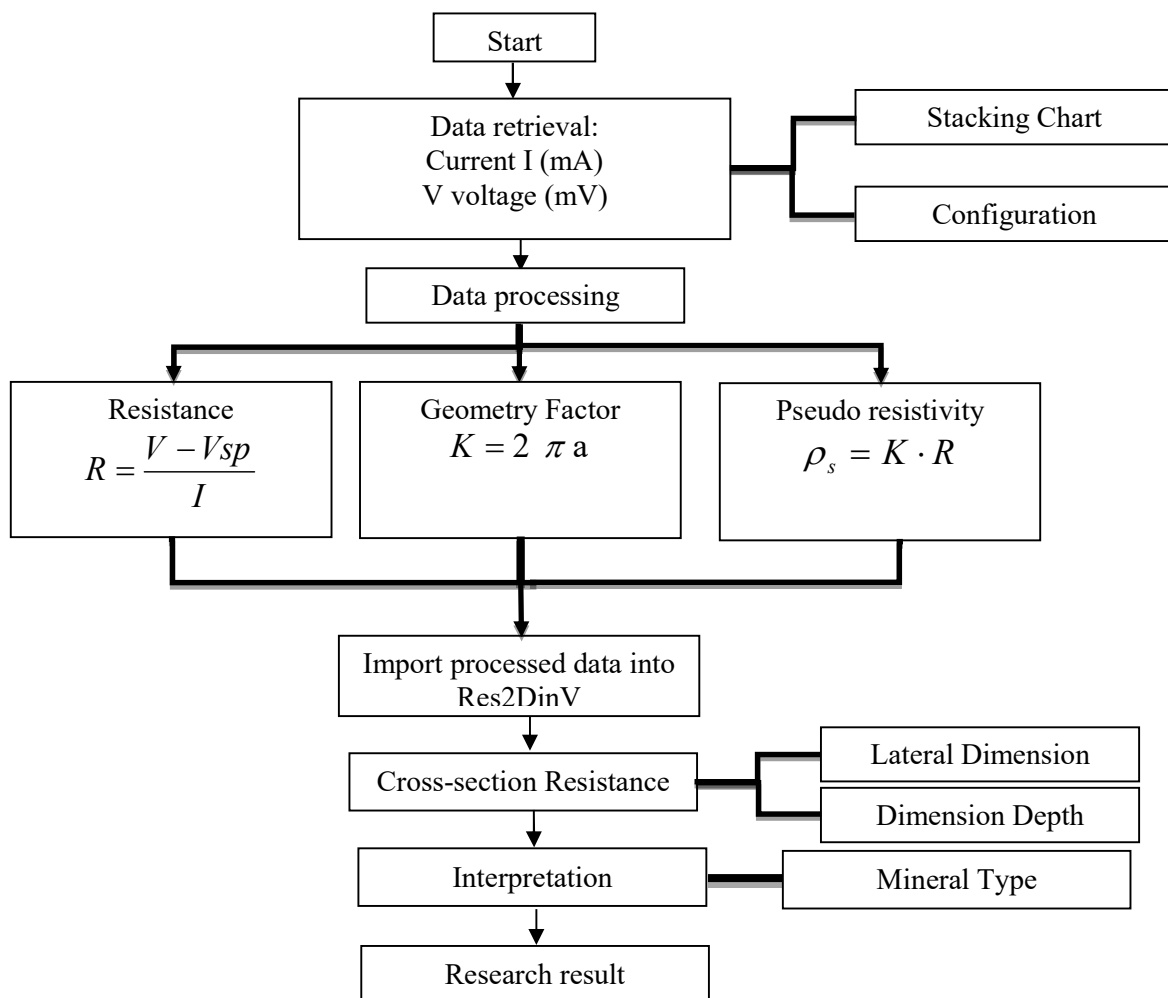


Figure 2. Research flow chart.

3. Result and Discussion

The results of measurements in the field obtained the value of voltage (V), strong current (I), the value of resistance (R), and the value of resistivity (ρ) as in table 1 below.

Table 1. Values of physical quantities from the field.

A	I (mA)	V (mV)	R (Ohm)	K	Apparent resistivity
3.00	1.74	0.37	0.21	18.80	4.01
3.00	1.27	0.17	0.13	18.80	2.52
3.00	6.60	0.18	0.03	18.80	0.51
3.00	6.06	0.16	0.03	18.80	0.49
3.00	5.78	0.14	0.02	18.80	0.46
3.00	5.51	0.15	0.03	18.80	0.51
3.00	5.50	0.05	0.01	18.80	0.17
3.00	5.50	0.01	0.00	18.80	0.03
3.00	5.12	0.16	0.03	18.80	0.59
3.00	4.77	0.09	0.02	18.80	0.36
3.00	4.27	0.03	0.01	18.80	0.13
3.00	3.78	0.04	0.01	18.80	0.19
3.00	5.12	0.16	0.03	18.80	0.59
6.00	3.54	0.08	0.02	37.70	0.85
6.00	4.52	0.29	0.06	37.70	2.42
6.00	4.04	0.22	0.05	37.70	2.05
6.00	6.06	0.05	0.01	37.70	0.31
6.00	5.78	0.05	0.01	37.70	0.33
6.00	5.51	0.19	0.03	37.70	1.29
6.00	5.50	0.27	0.05	37.70	1.85
6.00	5.50	0.35	0.06	37.70	2.39
9.00	5.12	0.12	0.02	56.50	1.33
9.00	4.77	0.65	0.14	56.50	7.70
9.00	4.27	0.15	0.04	56.50	1.99
9.00	3.78	0.68	0.18	56.50	10.17
9.00	3.54	0.71	0.20	56.50	11.34
12.00	4.52	0.21	0.05	75.40	3.50
12.00	4.04	0.65	0.16	75.40	12.12

The values obtained in Table 1 show the variation in values of each physical quantity. The amount of physical value variation obtained will directly affect the apparent resistivity (ρ) value obtained. The value of voltage (V) obtained is in the range (0.01-0.71) mV, while the value of electric current (I) is in the range (1.27-6.06) mA. For the value of resistance, R is in the range (0.01-0.21) Ω with the geometry factor k in the range 18.8-75.4, resulting in resistivity in the value range (0.03425-12.125) Ωm . The values in table 1 above are then processed in Res2dinV software to produce a resistivity cross-section, as shown in figure 3.

Figure 3 shows that the measurement length is 40.0 m with a depth of around 6.0 m. From the surface to a depth of about 4.0 m, it appears that the dominant minerals are hematite and magnetite and a little clay material with a resistivity of around 0.04 to 0.80 Ωm . Different from depths of 4.0 m to 6.0 m with resistivity around 1.72 to 7.99 Ωm , the dominant material is clay material.

Existing values indicate the corresponding range of values so that the geological conditions in interpreting also play an important role. The resistivity value (ρ) is not single, because as is known the subsurface material is not homogeneous and tends to mix with other materials. The type of material at the measurement location can be described as in table 2.

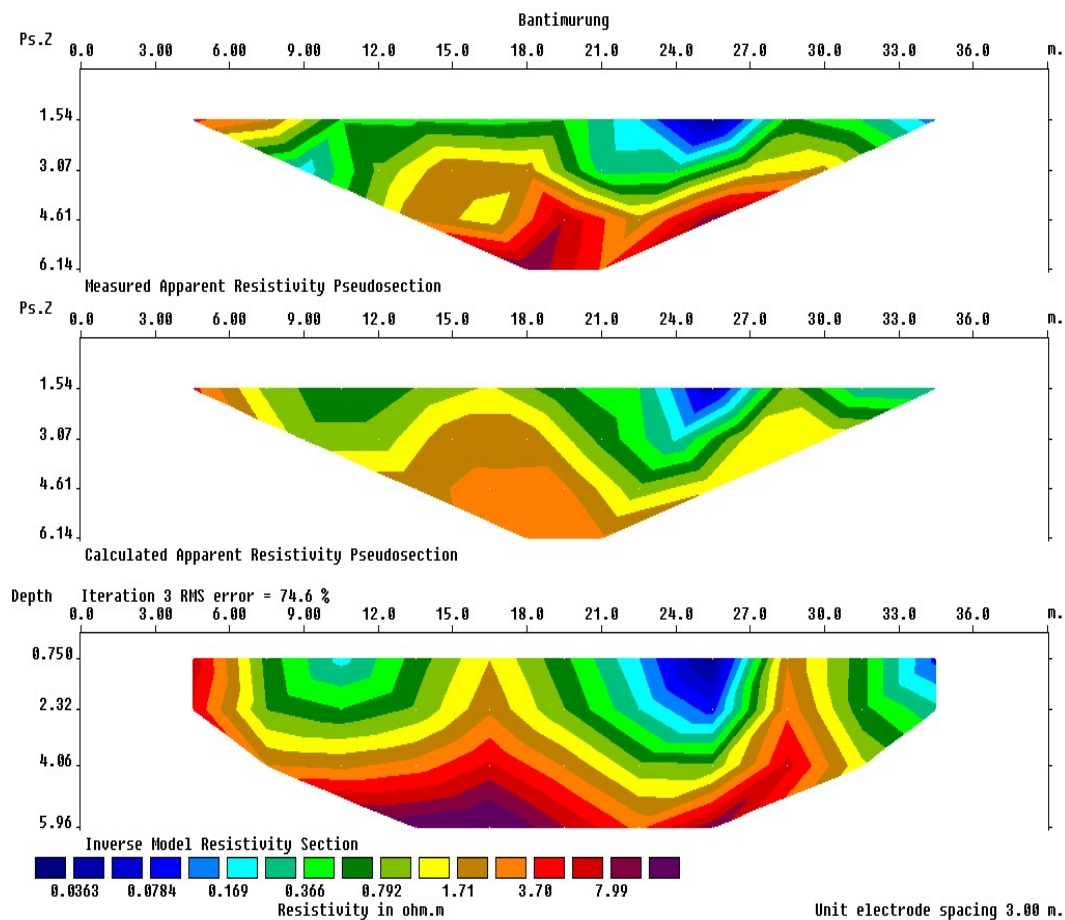








Figure 3. Cross-section of the resistivity model.

Table 2. Types of materials in the study area.

No	Colour	Resistivity (Ω m)	Material Type
1		0.17	Groundwater, sand, clay, and limestone
2		0.37	
3		0.79	
4		1.71	
5		3.78	
6		7.99	

From table 2 above, it can be seen that the resistivity value is in the range of 0.17 μ m to 7.99 μ m and the corresponding types of material are groundwater, sand, clay, and limestone. For types of minerals that correspond to the value of resistivity and type of material in the former mining area can be seen in table 3.

From table 3 it can be seen that the dominant minerals in the former mining area are chalcopyrite, galena, pyrite, pyrrhotite, magnetite, cassiterite, hematite, which are dominated by magnetite, pyrite and clay minerals.

Table 3. Types of minerals in the former mining area.

No	Resistivity (Ωm)	Minerals
1	0.04-0.08	Chalcopyrite, Galena, Pyrite, Pyrrhotite, Magnetite, Cassiterite
2	0.08-0.17	Hematite, Pyrite, Magnetite, Chalcopyrite, Cassiterite
3	0.17-0.37	Hematite, Magnetite, Cassiterite
4	0.37-0.79	Magnetite, Cassiterite
5	0.79-1.71	Clay, Magnetite, Cassiterite
6	1.71-3.77	Clay, Magnetite, Cassiterite
7	3.77-7.91	Clay, Magnetite, Cassiterite

Karst area has an attraction for investors. Its natural wealth is very diverse [6], both those that are above the surface, even more so below the surface. Natural resources on the surface ranging from flora to the types of fauna that live in karst areas [7-8]. This type of flora is very unique and has its community that is difficult to find in other regions. The wealth of flora will provide biodiversity to be preserved and remain preserved. While the fauna starts from the animals that live and develop in the cave to the fauna that inhabit the forest area [9]. The types of animals that live and develop have unique characteristics and tend to degrade from year to year [10].

Wealth below the surface, not only includes the type of cave ornaments that are often found, such as stalactite, stalagmite, hornblende, and others, but also other wealth in the land. The limestone mineral wealth and water resources available throughout the year are large capital that attracts investors. As a result, karst areas are very vulnerable to external pressure due to exploration and land use that is not by following per under the carrying capacity of the area.

The water stored in the cave becomes capital and a big advantage for capital owners to make it an economic commodity. On another aspect, the arrival of investors, both small and large scale, puts pressure on the karst region. The heterogeneous and fragile nature of the medium will easily change, in the form of the mineral hematite [11], magnetite [12-15], and clay into other minerals. Every change, both physical changes, and chemical changes will change the composition of rocks that form karst [16].

Clay material in the karst region becomes dominant because the physical properties of the medium are composed of limestone. As a result of rainfall that wet the surface, there will be a dissolution that will slowly but surely change the structure of the rock. Changes in rock structure can cause rocks to experience changes in physical properties, which have an impact on the mineral properties. Physical changes to minerals include crystal form, cleavage, hardness, colour, texture, and specific gravity.

The magnitude of clay density in the karst area of Maros for subsurface characteristics around depth to 15.70 m at a value of 279-1,612 Ωm , the type of material in the form of sand, clay, siltstone, surface water, and groundwater. Value of 1,612–6,196 Ωm for types of quartz, granite, basalt, and limestone. Value of 15,360–388,554 Ωm for rock salt and andesite materials. While the permeability value for 6 samples in a row is 0.948 D, 0.925 D, 0.841 D, 0.442 D, and 0.724 D [16].

Further research conducted by [17] on soil sample tests around Rammang-Rammang Karst Maros Region gives the results of the sequence The dominant molar oxides are SiO_2 (39.55 ± 1.97) wt.%, Al_2O_3 (27.72 ± 1.78) wt.%, FeO (10.81 ± 0.76) wt.% and SO_3 (10.25 ± 0.48) wt.%, while the order of atomic values is seen in these soil samples are silicon 14.28 at.%, aluminum 11.80 at.%, iron 3.26 at.% and sulfur 2.78 at.%.

4. Conclusion

Profile of sedimentary layers in the former mine area of the Karst Maros area in the form of resistivity measurement results with bedding at the lowest to highest resistivity values respectively are 0.17 Ωm to 7.99 Ωm and types appropriate materials are groundwater, sand, clay, and limestone. The varying

resistivity value is around a depth of up to 6 m. After this depth, the bedding will have almost the same material in the form of hard limestone. The composition of sediment minerals in the former mining area of the Maros karst area consists of chalcopyrite, galena, pyrite, pyrrhotite, magnetite, cassiterite, hematite, and clay.

5. References

- [1] Williams D F 1989 *Karst Geomorphology and Hydrology*. London: Chapman and Case Studies.
- [2] Arsyad M, Ihsan N, Tiwow V A 2016 *AIP Conf. Proc.* **1708**, 070003.
- [3] Fatmainnah, Arsyad M, and Palloan P 2018 *J. Phys.: Conf. Ser.* **1120** 012057.
- [4] Haryono E 2001 *Nilai Hidrologi Bukit Karst*. Yogyakarta: Makalah di Fakultas Teknik Sipil UGM .
- [5] Ludman A, and Nicholas K Coch. 1982 *Physical Geology*. McGraw-Hills: USA, p: 362-481.
- [6] Barkey R, Nursaputra M, Mappiase M F, Achmad M, Solle M, and Dassir M 2019 *IOP Conf. Ser.: Earth Environ. Sci.* **235** 012022.
- [7] Hiola S F, Dirawan G D, Wiharto M, and Syamsiah 2019 *IOP Conf. Ser.: Mater. Sci. Eng.* **551** 012132.
- [8] Ansari F, Jeong Y, Putri I A, and Kim S 2019 *J. Sustainability* **11**(6) 1789.
- [9] Barkey R, Nursaputra M, and Mappiase, M. F. 2019 *IOP Conf. Ser.: Earth Environ. Sci.* **270** 012007.
- [10] Duli A, Mulyadi Y, and Rosmawati 2019 *IOP Conf. Ser.: Earth Environ. Sci.* **270** 012014.
- [11] Fahlepy M R, Wahyuni Y, Andhika M, Tiwow V A, and Subaer 2019 *Materials Science Forum* **967** 259-266.
- [12] Tiwow V A, Arsyad M, Palloan P, and Rampe M J 2018 *J. Phys.: Conf. Ser.* **997** 012010.
- [13] Fahlepy M R, Tiwow V A, and Subaer 2018 *J. Phys.: Conf. Ser.* **997** 012036.
- [14] Arsyad M, Tiwow V A, and Rampe M J 2018 *J. Phys.: Conf. Ser.* **1120** 012060.
- [15] Tiwow V A, Arsyad M, Sulistiawaty, Rampe M J, and Tiro W I B 2019 *Materials Science Forum* **967** 292-298.
- [16] Arsyad M, Pawitan H, Sidauruk P, and Putri E I K 2014 *J. Manusia & Lingk.* **21**(1) pp.8-14.
- [17] Sulistiawaty, Arsyad M, and Tiwow V A 2015 Proc. HFI Symposium Fisika Bali, Denpasar pp.219-226.

Acknowledgments

This research can be carried out not only because of good cooperation between the implementation team but also for the help of various parties. Thank you to the Chancellor and Dean of FMIPA for providing PNPB funds and Earth Physics students for their willingness to help the research team in obtaining data and analyzing it.

● **8% Overall Similarity**

Top sources found in the following databases:

- 8% Internet database
- 0% Publications database
- Crossref Posted Content database

TOP SOURCES

The sources with the highest number of matches within the submission. Overlapping sources will not be displayed.

1	123dok.com Internet	3%
2	repository.unhas.ac.id Internet	2%
3	elibrary.kdpu.edu.ua Internet	1%
4	sinta.ristekbrin.go.id Internet	<1%
5	sinta3.ristekdikti.go.id Internet	<1%
6	d289ngcuqcswqg.cloudfront.net Internet	<1%

● Excluded from Similarity Report

- Crossref database
- Bibliographic material
- Cited material
- Manually excluded sources
- Submitted Works database
- Quoted material
- Small Matches (Less than 10 words)

EXCLUDED SOURCES

researchgate.net	9%
Internet	
iopscience.iop.org	8%
Internet	
repository.lppm.unila.ac.id	7%
Internet	
eprints.unm.ac.id	7%
Internet	
jglobal.jst.go.jp	1%
Internet	